Progress in Nuclear Energy 96 (2017) 62–75

Contents lists available at ScienceDirect

Progress in Nuclear Energy

journal homepage: www.elsevier.com/locate/pnucene

External heat transfer capability of a submerged SMR containment: The Flexblue case

M. Santinello [a], M.E. Ricotti [a, *], H. Ninokata [a], G. Haratyk [b], J.J. Ingremeau [b], V. Gourmel [b]

[a] Politecnico di Milano, Dept. of Energy, CeSNEF-Nuclear Engineering Division, Via La Masa 34, 20156, Milano, Italy
[b] DCNS, 40-42 rue du Docteur Finlay, 75015, Paris, France

ARTICLE INFO

Article history:
Received 17 January 2016
Received in revised form
17 November 2016
Accepted 1 December 2016

Keywords:
SMR
Subsea-based
Transportable
Passive safety
CFD

ABSTRACT

Flexblue® is a 160 MWe, transportable and subsea-based nuclear power unit operating up to 100 m depth several kilometers away from the shore. The concept is based on existing technologies and experience from the oil&gas, civil nuclear and shipbuilding industries. In a post-Fukushima world, its safety features are particularly relevant. The immersion provides inherent protection against most external aggressions including tsunamis, extreme weather conditions and malevolent actions. The vicinity and the availability of an infinite, permanent heat sink – the ocean – enhances the performance of the safety systems which, when designed to operate passively, considerably extend the grace period given to operators in case of accident. The present work investigates seawater natural convection fluid dynamics and heat transfer features, induced by the heating of Flexblue® reactor containment, to evaluate the capabilities of the system to reject the decay power to the exterior in case of an accident. A preliminary lumped parameters approach has been adopted, revealing that the large diameter of the hull (14 m) is such that ranges of validity of empirical correlations for natural convection heat transfer are always exceeded and conditions for their correct application are not satisfied. Hence, a 2D, unsteady CFD analysis has been performed to simulate the natural convection flow in the ocean, thus obtaining predictions for heat flux distribution, hull superficial temperature profile and heat transfer coefficient. Both CFD sensitivity and parametric analyses have been carried out, even if within a 2D approach, to limit the computational burden. The results showed that the heat transfer process is globally satisfactory to ensure the safe cooling of the reactor. A 3D approach and an experimental campaign aimed at validating the CFD results have been planned.

1. Introduction

The current offer of nuclear power plants (NPPs) is mainly composed of large-scale units rated at more than 1000 MWe. These units fit well to the needs of large power grids such as in Europe or China, where big utilities can afford the initial investment required for the construction. However, these units do not fit well in smaller grids, where they would represent more than 10% of the installed capacity. They underestimate the difficulties of utilities to afford large investments, and the related high premium that bankers and investors demand on such projects, where cost and delay overruns are common (Kessides, 2012; Thomas, 2012). In consequence, the financing of a large nuclear reactor is complicated for most utilities. The competition with fossil-fueled units and, in some areas, with renewable energies, is harsh.

To address these challenges, the nuclear industry is today developing small modular reactors (SMRs) (Vujic et al., 2012). SMRs would facilitate the financing thanks to a more progressive investment, a shorter construction time and an accelerated return on investment (Rosner and Goldberg, 2011). The Levelized Cost of Electricity (LCOE) of SMRs compensates the 'economies of scale' by 'economies of number' and by simplifying the reactor design (Boarin et al, 2012; Lokhov et al, 2011). Yet these units' cost still suffers from significant civil work, since reactors are often bunkered underground (Xie, 2012).

Besides, there happens to be significant energy needs in regions of the world where land is scarce, isolated or just unsuitable for the construction of a nuclear reactor. This is for instance the case of

* Corresponding author.
E-mail addresses: marco.santinello@polimi.it (M. Santinello), marco.ricotti@polimi.it (M.E. Ricotti), hisashi.ninokata@polimi.it (H. Ninokata), gharatyk@mit.edu (G. Haratyk), jeanjeacques.ingremeau@dcnsgroup.com (J.J. Ingremeau), vincent.gourmel@dcnsgroup.com (V. Gourmel).

http://dx.doi.org/10.1016/j.pnucene.2016.12.002

remote areas with large natural resources, islands or highly populated areas under the threat of natural hazards. Transportable offshore nuclear power plants, such as the floating barge Akademik Lomonosov (Kuznetsov, 2012) aim at addressing the first case. This barge, under construction in Russia, will be supplying North-East Siberia in energy without the need for frequent refueling in gas, as it is the case today.

An alternative solution to the floating transportable plant consists in setting the reactor underwater, on the seafloor. Electric Boat (General Dynamics Electric Boat Division, 1971) and J. S. Herring, (1993) investigated such subsea reactor designs in the 1970's and 1990's respectively. These projects stayed at the paper project stage. The progress in subsea oil&gas technologies, submarine cables for offshore renewables and in shipbuilding techniques make offshore power reactors more feasible today than before, with an increasing interest towards that option (Buongiorno et al., 2016). They appear attractive as the Fukushima accident calls our nuclear industry to better consider extreme external events in the design of NPPs.

Based on its experience in the design, fabrication, maintenance and dismantling of nuclear-powered submarines and ships, DCNS is developing a subsea, transportable nuclear power plant named Flexblue®.

2. The Flexblue® concept

2.1. Module main features

Flexblue® is a subsea and fully transportable modular power unit (Haratyk et al., 2014). It supplies 160MWe to the grid via submarine cables. It is immersed down to a hundred meter depth, a few kilometres away from the shore, within territorial waters (Fig. 1).

Flexblue® is entirely manufactured in factories and assembled in a shipyard per naval modular construction techniques. The module, a cylindrical hull of about 150 m long and 14 m diameter, is brought on site by transport ship and moored on the seafloor, where production takes place. The module is monitored, protected but also possibly operated from an onshore control center. It is permanently accessible via a submarine vehicle that connects to access hatches, so that light maintenance, inspection and operation can be performed onboard while on the seafloor.

Every 3 years approximately, electricity production stops for refueling. The module is removed and transported back to a coastal facility, which hosts the spent fuel pool.

Major overhaul occurs every 10 years, i.e. every three fuel cycles. Several Flexblue® units can operate on the same site and hence share the same support systems. The main characteristics and reactor data of a Flexblue® unit are listed in Table 1.

Flexblue® uses typical pressurized water reactor technology, which benefits from a considerable experience in commercial power plants and naval environments. The reactor utilizes only civil proven technologies: although adaptation of components to the particular design is required, no innovative or risky development is expected.

DCNS and its partners are currently considering different types of reactors: a loop-type design called ‘reference design’ is presented here for illustration purpose. The reference design exhibits two primary loops: two primary coolant pumps and two recirculation steam generators. The main safety and auxiliary fluid systems are located in the reactor section and the turbine section. In addition to the reactor section, the Flexblue® module hosts the turbine & alternator section, the aft section and the fore section. These two latter sections accommodate: emergency batteries, a secondary control room, process auxiliaries, I&C control panels, spares, living areas for a crew, and emergency rescue devices.

Redundant main and auxiliary submarine cables transport electricity as well as information between the module and the onshore control center.

2.2. Safety, security and environment

The Flexblue® concept not only complies with the latest European safety standards (Generation III + reactors) but also offers room for significant breakthroughs in nuclear safety. The safety of Flexblue® indeed benefits from its manufacturing process and from the submerged environment at several levels. Firstly, the quality of manufacturing in a factory is enhanced. Secondly, most external hazards, whether they are natural or from human actions, are diminished underwater. Extreme weather conditions (e.g. wind, storms, snow, floods, drought, heat waves), tsunamis, earthquakes (thanks to appropriate engineering features) have no or little impact on the plant. Last but not least, the availability and infinity of the heat sink, in relation with passive safety systems, provides a long and efficient performance of the reactor safety functions without need for external power. The likelihoods of core damage and large early release of radioactivity are extremely low.

The reactor containment (reactor sector) is bounded by the hull on the sides and the reactor sector walls on the front and on the back (Fig. 2). A large share of the metal containment walls are therefore in direct contact with seawater, which provides very efficient containment cooling without the need for containment spray or cooling heat exchanger. This paper actually focuses on the external side of heat transfer and shows the potentiality of such concept.

Two large tanks of water – the safety tanks – act as intermediate heat sinks, as pressure suppression pools (like in BWRs) and/or as sources of coolant injection depending on the accident scenarios.

In case of an accident, active systems are used if AC power is available. If not, passive safety systems are actuated automatically when emergency set points are reached. The passive safety strategy is based on reaching a safe shutdown state via passive means. As an example, in case of Loss Of Flow Accidents (LOFA), the reactor is shutdown and natural convection closed loops activate to provide emergency core cooling, to transfer decay heat to the environment: emergency heat exchangers both on the primary side (immersed in the safety tanks) and on the secondary side (directly immersed into seawater) are available. In case of LOCA scenarios, several cold water injection sources restore core coolant inventory: core make-up tanks at high pressure, accumulators at medium pressure and gravity driven safety tanks at low pressure. Low primary pressure is achieved through automatic depressurization system. Condensation occurs on the containment walls. Once gravity injection tanks empty, recirculation sump screens actuate to collect the condensates at the bottom of the containment and reinject them into the core. No pump is required and heat is ultimately evacuated through the containment walls to the environment.

The large surface area of the naturally-cooled containment wall in contact with seawater ensures very efficient heat removal, as this study will show. Sump pH control and inertisation prevent containment damage from corrosion and hydrogen flammability respectively.

The containment is designed to sustain even severe accidents with core meltdown. In this case, the mitigation strategy consists in in-vessel corium retention assisted by an ex-vessel passive core cooling. In the unlikely catastrophic hypothesis where all barriers would have failed, radioactive elements would be released into seawater. However, unlike an atmospheric release of a land-based reactor (Ramana et al, 2013), no short-term emergency counter

Fig. 1. Flexblue® plant layout.

measures would be needed, to protect the population against direct exposure. Specific measures would only be required to protect the environment and control the food chain, in a limited time and space frame. Safe re-containment and retrieval of the entire nuclear station would be possible for later dismantling in a dedicated facility.

3. Drywell fluid dynamics features

3.1. External hull heat transfer: lumped parameters approach – cylindrical approach

The main goal of this study is to investigate the fluid dynamics of the external water in natural convection around the hull. As a first step, a classical analysis was performed, using a lumped parameters approach: the heat transfer process was modeled with an equivalent electrical scheme (Fig. 3), considering both the thermal conduction across the containment and seawater natural convection. Contributions to the total thermal resistance of the containment are given by the carbon steel thickness of the cylinder, the painting layer and the biofouling sediment.

The painting and the fouling layers have a low thermal conductivity, thus they increase the resistance to heat transfer and reduces the effectiveness of hull heat exchanger. For painting thermal conductivity, a wide range of literature data are available and the generic value 0.3 W/mK is used. Determination of biofouling properties is a more difficult task. In literature, it is known that typical fouling resistances are roughly 10 times lower in plate heat exchangers than in shell-and-tube heat exchangers (Awad, 2011). Awad (Awad, 2011) suggests that a usual value for the thermal resistance of a plane biofouling layer in seawater is 2.6e-05 m2K/W. In contrast, Pugh et al. (2003) provide a distinction between oceanic and costal seawater, recommending the values 2.6e-05 m2K/W and 4.3e-05 m2K/W respectively. The latter of the mentioned values is here used.

Five empirical correlations available in open literature for natural circulation heat transfer from a long horizontal cylinder were evaluated (see Appendix A). The model assumes a uniform hull internal temperature equal to 100 °C and a high seawater temperature equal to 35 °C. Calculations for Rayleigh number, hull superficial temperature, heat flux and heat transfer coefficient are shown in Table 2. The results reveal that, due to the large diameter of the Flexblue® hull, the configuration of interest falls outside the range of validity of all the correlations (Fig. 4): the extrapolation of the correlations beyond their limit of validity puts in an uncertain situation, hence a CFD approach is needed.

3.2. External hull heat transfer: lumped parameters approach – planar approach

Since the cylindrical approach turned out to be problematic because of the large diameter of the reactor containment, another type of approach, dealing with smaller surfaces, has been attempted. The planar approach consists of an approximation of the circular shape of the reactor containment with an octagon having the same perimeter. The use of correlations for natural convection from planar surfaces is made within their limits of validity. However, a very strong hypothesis is necessary for this type of approach: insulated surfaces must be considered, neglecting the interaction between neighboring surfaces.

In the configuration shown in Fig. 5, it is important to make a distinction among the possible configurations of the plate, depending on the angle between the force of gravity and the temperature gradient. Five cases are possible: horizontal plate upper surface heated, inclined plate upper surface heated, vertical plate, inclined plate bottom surface heated, horizontal plate bottom surface heated. Several correlations are adopted for the different uses (McAdams, (1954), Churchill & Chu (Churchill and Chu, 1975b), Fujii & Imura (McAdams, 1954; Fujii and Imura, 1972) Raithby & Hollands (Raithby and Hollands, 1998), Kitamura & Kimura (Kitamura and Kimura, 1995), Kozanoglu & Lopez (Kozanoglu and Lopez, 2007), Clausing & Berton (Clausing and Berton, 1989)). Results of the planar approach are shown in Table 3.

3.3. CFD analysis and results

In the preliminary CFD analysis, a 2-D geometry is adopted. Constant boundary conditions are assumed: 1 bar internal condensing steam, 100 °C internal wall surface temperature, a conservative value of 35 °C external temperature of the sea, uniform thickness and thermal conductivity of the hull wall, including thermal resistances due to paint layer and biofouling. Stagnant seawater is assumed, i.e. the possible presence of sea currents is ignored. The hull is suspended at a given distance from the seabed and entirely surrounded by seawater.

Table 1
Flexblue® main characteristics and reactor data.

Parameter	Value	Parameter	Value
Unit power	160 MWe	Reactor core	77 fuel assemblies
Thermal power	530 MWth	Fuel assembly	17 × 17 rods
Length	150 m	Active length	2.15 m
Diameter	14 m	Enrichment	<5%
Displacement	16 000–20 000 MT	Average power density	~70 kW/L
Immersion depth	Up to 100 m	Primary pressure	15.5 MPa
Cycle length	40 months	Delta T core	30 °C
Lifetime	60 years	Core mass flow rate	~3160 kg/s
Steam Gen.	Recirculation	Number of loops	2
Steam Gen. pressure	62 bars (saturated, hot full power)		

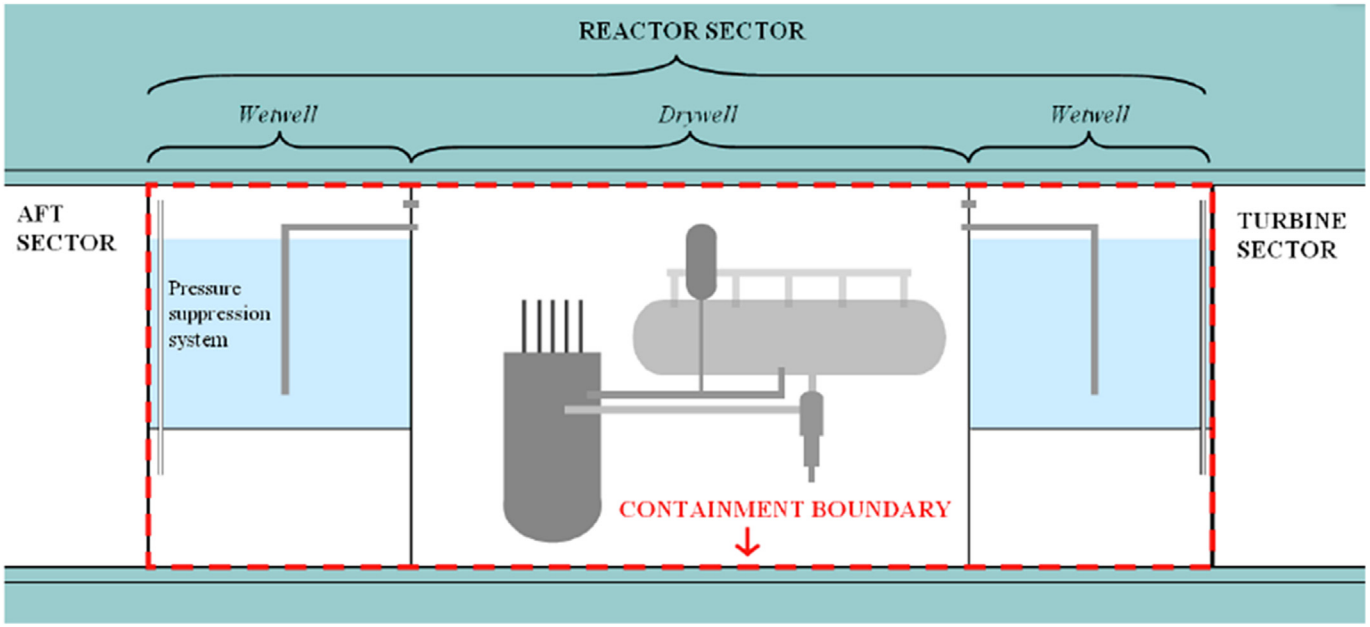

Fig. 2. The reactor sector boundary (drywell and wetwell) with its safety water tanks.

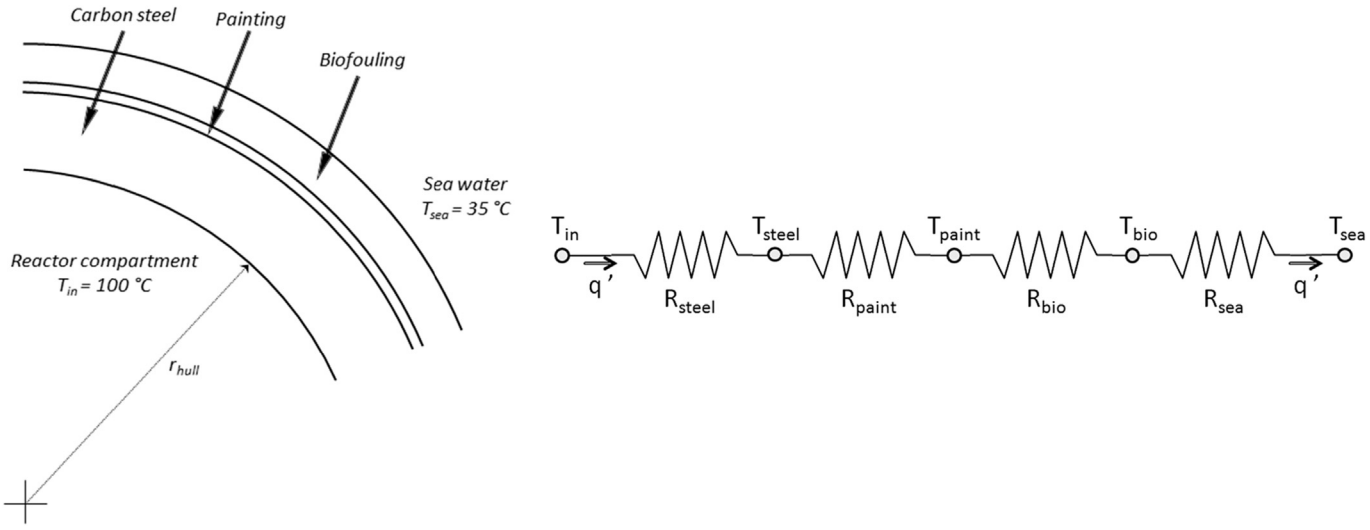

Fig. 3. Hull-drywell containment system and equivalent electrical scheme (heat transfer).

Table 2
Results of the conductive-convective problem using five different correlations.

Author	Range of validity	Heat Flux [W/m^2]	$T_{w,ext}$ [K]	h_{ext} [W/m^{2}K]	Rayleigh number
Morgan (Morgan, 1975)	$10^{-2} < Ra_D < 10^{12}$	4.82e+05	325.70	620.67	1.42e+15
Churchill & Chu (Churchill and Chu, 1975a)	$Ra_D < 10^{12}$	4.86e+05	325.30	640.57	1.39e+15
Heo & Chung (Heo and Chung, 2012)	$1.69 \times 10^8 < Ra_D < 5.07 \times 10^{10}$	4.03e+05	333.45	360.17	2.05e+15
Raithby & Hollands (Raithby and Hollands, 1998)	Rayleigh number zone uncertain	4.66e+05	327.25	551.61	1.55e+15
Sedahmed & Shemilt (Sedahmed and Shemilt, 1982)	$1.9 \times 10^{10} < Ra_L < 3.8 \times 10^{11}$	4.25e+05	331.29	415.45	1.88e+15

The analysis is aimed at computing heat flux and temperature distributions on the external surface of the hull as an angular function (0°–360°), to estimate local and global heat transfer coefficient. An unsteady simulation is performed, so that typical plume oscillations of natural circulation flow can be observed.

3.3.1. Geometry and mesh

A large portion of ocean (300 m width i.e. 10 times the hull dimension on both sides, 60 m depth) is simulated, to avoid wall effects on the velocity field near the hull. The hull is placed 6 m above the seafloor. A very fine mesh is structured in the region near the hull, while an unstructured coarse and very coarse mesh is built

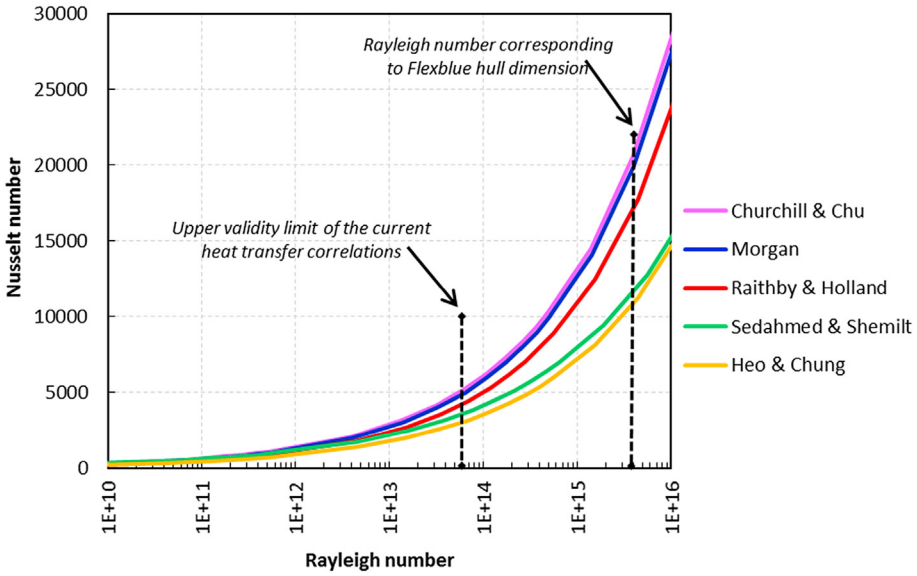

Fig. 4. Average Nusselt number as a function of the global Rayleigh number.

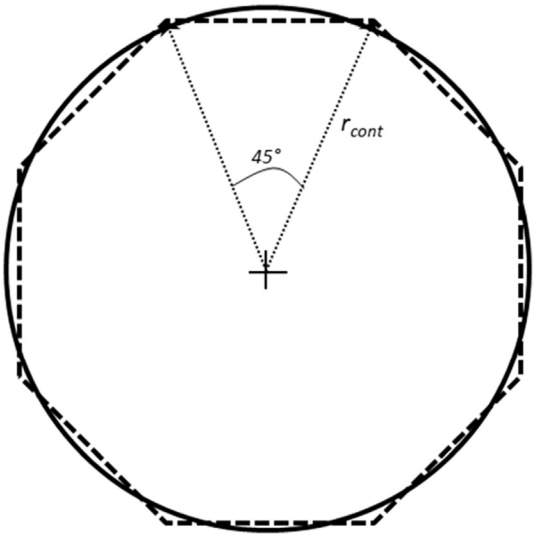

Fig. 5. Approximation of the circle with an octagon.

in the remaining part of the geometry (see Fig. 6 and Table 4). Nearly 400 000 square cells are located in 1 m wide annulus around the hull (near wall zone), half of which lies in the 0.2 m wide region (boundary layer zone), with at least one node in the viscous sublayer ($y^+ \leq 5$) and several nodes in the buffer and turbulent zones.

3.3.2. Physical modeling and solver

Unsteady incompressible Navier-Stokes and energy balance equations are adopted and solved with approximations. ANSYS FLUENT 14.0 code is adopted for the numerical solution of the equations. The variation of properties due to the increasing temperature is dealt with Boussinesq assumption, since the condition $\beta(T - T_0) \ll 1$ is satisfied. Turbulence is modeled with the SST version of the k-ω model (Menter, 1994): it is often used in CFD natural circulation problems (Krepper et al., 2007; Ganguli et al., 2010; Jeong et al., 2009; Braga Vieira et al., 2010), since it combines the good near-wall behavior of the k–ω model with the robustness of the k–ε model in the far field in a numerically stable way. In ANSYS Fluent, opportune expressions for generation and dissipation terms are included in order to make turbulence equations consistent with Boussinesq assumption. The k-ω model

Table 3
Results of the planar approach.

		Heat Flux [W/m^2]	T_{steel} [K]	T_{paint} [K]	T_{bio} [K]	h_{sea} [W/m^{2}K]	Rayleigh number
Vertical surface	Average	1.07e+04	361.48	326.92	326.46	586.31	9.00e+13
	Standard deviation	3.46e+02	0.35	1.50	1.51	66.66	7.45e+12
	%	3.24	0.39	2.79	2.84	11.37	8.27
Inclined plate upper surface heated ($\theta = 45°$)	Average[a]	1.14e+04	361.75	323.75	323.26	754.37	7.43e+13
Horizontal plate upper surface heated	Average	1.11e+04	362.04	325.02	324.55	680.54	6.34e+13
	Standard deviation	2.46e+02	0.25	1.07	1.08	58.48	3.42e+13
	%	2.21	0.28	2.05	2.09	8.59	53.85
Inclined plate bottom surface heated ($\theta = 45°$)	Average	1.04e+04	354.76	328.15	327.70	534.58	6.80e+13
	Standard deviation	3.63e+02	0.36	1.57	1.59	61.31	5.53e+12
	%	3.49	0.41	2.86	2.91	11.47	8.13
Horizontal plate bottom surface heated	Average	4.16e+03	368.99	355.14	354.96	90.73	1.10e+14
	Standard deviation	1.19e+03	1.19	5.14	5.19	35.41	1.44e+14
	%	28.56	1.24	6.27	6.35	39.03	130.80
Overall planar approach	Average	1.18e+04	363.13	329.72	329.29	565.22	–
	Standard deviation	1.03e+03	1.03	4.47	4.52	190.34	–
	%	8.47	1.36	8.10	8.24	32.10	–

[a] Only one correlation available for that case.

Table 4
Grid data (2-D simulation domain: 60 m depth × 300 m length).

Zone	Area [m^2]	Number of cells	Mesh type	Refining
Boundary layer	8.98	200 000	Structured	Very fine
Near wall	35.86	200 000	Structured	Fine
Plume and near hull seawater	1601.3	322 000	Unstructured	Coarse
Far away seawater	16 200	55 000	Unstructured	Very coarse

makes use of the "so-called" enhanced wall treatment. The enhanced wall treatment is a method to define profiles of momentum and energy, which can extend its applicability throughout the near-wall region (i.e., viscous sublayer, buffer region, and fully-turbulent outer region). It consists of a single wall law for the entire wall region, made through a blending between the linear law of the viscous sublayer and the logarithmic law of the fully-turbulent region. Functions suggested by Kader, (1981) for momentum and energy equations are used. For details about modeling of turbulence and natural circulation, the authors refer to ANSYS Fluent theory guide (Theory Guide, 2011). Governing equations of the flow are here reported:

Continuity

$$\frac{\partial u}{\partial x}+\frac{\partial v}{\partial y}=0 \tag{1}$$

x - momentum

$$\rho\left(\frac{\partial u}{\partial t}+\mathrm{div}(u\ \mathbf{u})\right)=-\frac{\partial p}{\partial x}+\mu\nabla^2 u \tag{2}$$

y - momentum

$$\rho\left(\frac{\partial v}{\partial t}+\mathrm{div}(v\ \mathbf{u})\right)=-\frac{\partial p}{\partial y}+\mu\nabla^2 v+\rho_0 g(1-\beta(T-T_0)) \tag{3}$$

Energy

$$\rho c_p\left(\frac{\partial T}{\partial t}+\mathrm{div}(T\ \mathbf{u})\right)=K\nabla^2 T \tag{4}$$

Turbulent kinetic energy

$$\rho\left(\frac{\partial k}{\partial t}+\mathrm{div}(k\ \mathbf{u})\right)=\left(\mu+\frac{\mu_t}{\sigma_k}\right)\nabla^2 k+G_k-Y_k \tag{5}$$

Turbulence frequency

$$\rho\left(\frac{\partial \omega}{\partial t}+\mathrm{div}(\omega\ \mathbf{u})\right)=\left(\mu+\frac{\mu_t}{\sigma_\omega}\right)\nabla^2 \omega+G_\omega-Y_\omega \tag{6}$$

Second order upwind scheme in space and second order implicit method in time are used. Pressure term is treated with PRESTO! scheme and PISO algorithm is adopted for pressure velocity coupling. A total time of more than 8000 s is simulated. Constant and uniform temperature equal to 100 °C is kept on the internal surface of the hull. Thermal conduction across the containment is simulated taking into account the thermal resistances of the carbon steel layer and painting.

3.3.3. Results

The resulting temperature field is shown in Fig. 7. The heating of seawater outside the boundary layer is very small: only a little portion of the ocean feels the effect of the heating process and the temperature variation is almost lower than 1 °C. Ocean represents an infinite heat sink. Nearly 90% of temperature gradient lies in a 0.02 m width layer, while bulk temperature is reached at approximately 0.40 m from the hull (Fig. 8). Profiles for temperature and heat transfer coefficient on the outer surface of the hull are shown in Fig. 9. Two peaks can be noticed in the temperature plot, generated by flow stagnation near the top and the bottom of the hull. Therefore heat cannot be removed efficiently thus seawater temperature increases, resulting in lower heat flux. The heat transfer process in the upper hemisphere of the hull can be even three or four time more efficient with respect to the lower hemisphere, with the exception of the top of the hull where stagnation occurs due to plume formation.

CFD analysis allows the calculation of local quantities, while heat transfer correlations provide only a global value based on the assumption of uniform temperature distribution. Table 5 reports the comparison by means of average results. The exact way to obtain the average value of the heat transfer coefficient is given by the integral of the profile of the local heat transfer coefficient, divided by the amplitude of the domain of integration:

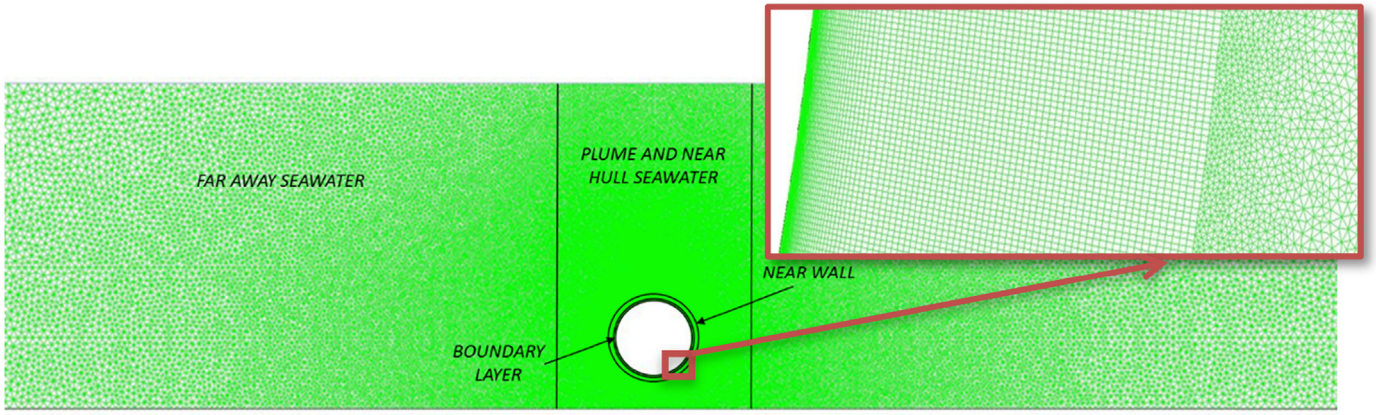

Fig. 6. Grid structure for the hull and seawater simulation.

$$\overline{h} = \frac{1}{2\pi}\int_0^{2\pi} h_L(\gamma)d\gamma \tag{7}$$

which is obviously calculated numerically, on the basis of the local values h_l in the cells adjacent to the wall:

$$h_L = \frac{q_1''}{(T_{wL} - T_\infty)} \tag{8}$$

CFD global values are averaged all along the hull surface (360°). A local approach is anyway more correct because the heat transfer on the hull is characterized by a non-uniform distribution of temperature and heat flux on the external surface. Discrepancies between CFD averaged results and min-max values obtained from the correlations justify the need of an experimental investigation of the Flexblue® hull, confirming that a simple extrapolation of the existing correlations is unreliable.

The velocity field (Fig. 10) shows the presence of an oscillating plume. It reveals also that the side walls of the grid are sufficiently far from the hull, so that the heat transfer process is not affected. The velocity boundary layer (Fig. 11) enlarges, as expected, from the lower to the upper part of the hull, from few cm to around 1 m. The seawater far away from the hull and from the plume regions moves very slowly.

The strange behavior of the profiles near the summit of the hull

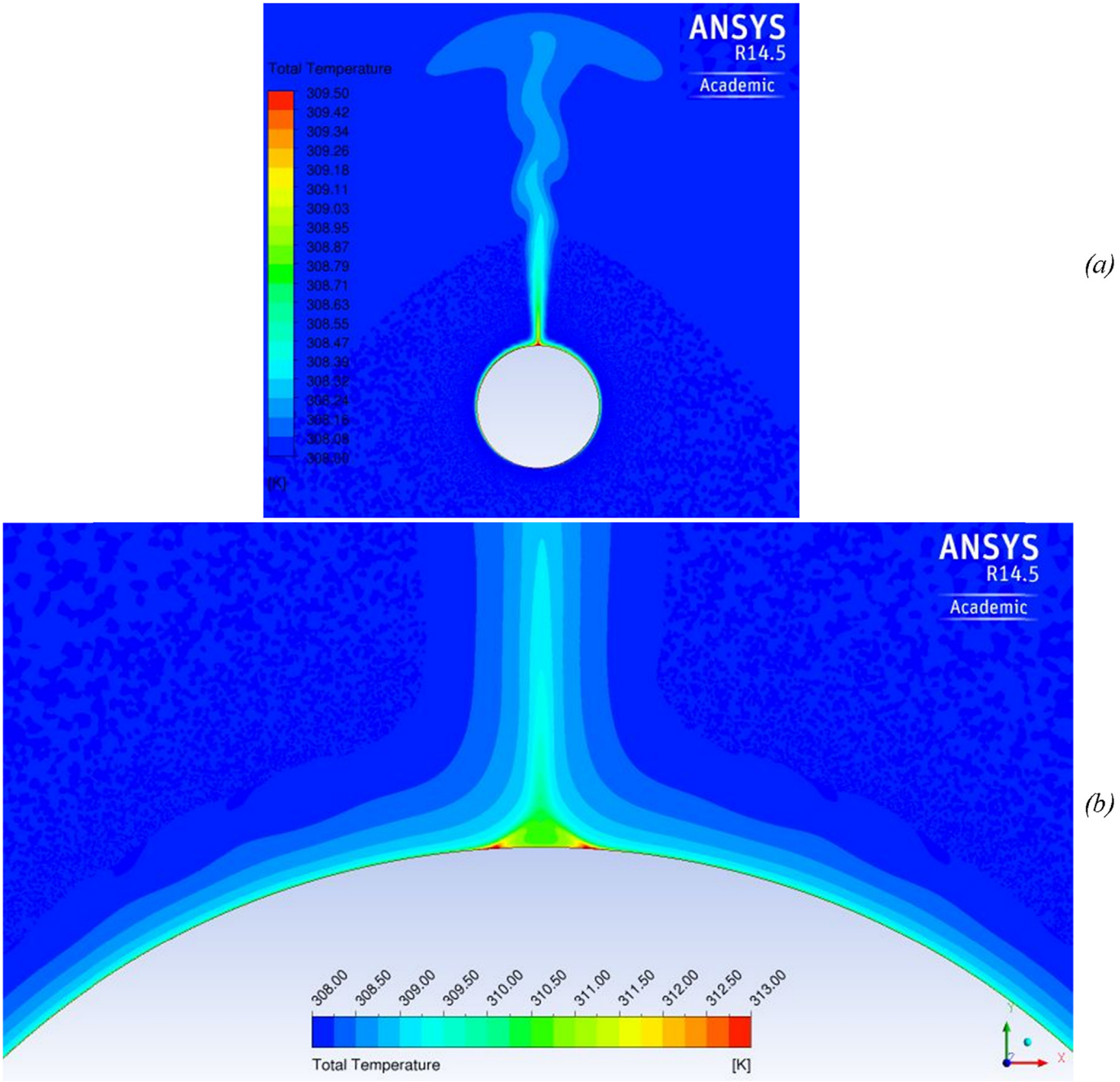

Fig. 7. Temperature field in seawater (a) and thermal boundary layer at the top of the hull (b).

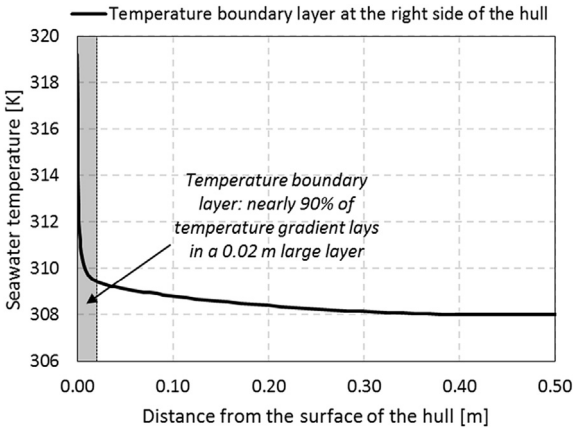

Fig. 8. Plot of the thermal boundary layer on the right side of the hull (at angle $\gamma = 0°$).

($\gamma \approx 90°$) is a result of the convergence of the two natural circulation flows coming from the left and the right side of the hull. This phenomenon generates a complex velocity field in this zone: separation of the boundary layer occurs only here. The two flows generate two small recirculation vortices, causing two stagnation points responsible of the two peaks that are visible near the position $\gamma = 90°$. In the middle of these two points, there is not stagnation, since the two recirculation vortices push water against the hull. This situation can be visualized in the velocity vectorial plot of Fig. 12. As noticeable, the velocity vectors near the position $\gamma = 90°$ are directed toward the hull surface. Nevertheless, despite the scientific interest of this behavior of the flow, its impact on the global heat transfer process is limited.

3.4. Sensitivity analysis

A sensitivity analysis was performed to assess the solidity of the CFD simulation. The sensitivity to mesh, to the numerical discretization schemes and to the turbulence models were investigated.

Table 5
Comparison between CFD study and lumped parameters analysis.

Quantity	CFD global mean values	Correlations values (cylindrical) min, avg, max	Discrepancy min, avg, max
Hull outer surface temperature [K]	326.2	325.3, 328.6, 333.4	−0.2, + 0.7, +2.1%
Heat flux [W/m^2]	10 686	9096, 10 200, 10 970	−14.8, −4.6, +2.6%
Heat transfer coefficient [W/m^{2}K]	670.7	360.1, 517.7, 640.5	−46.3, −25.7, −4.5%

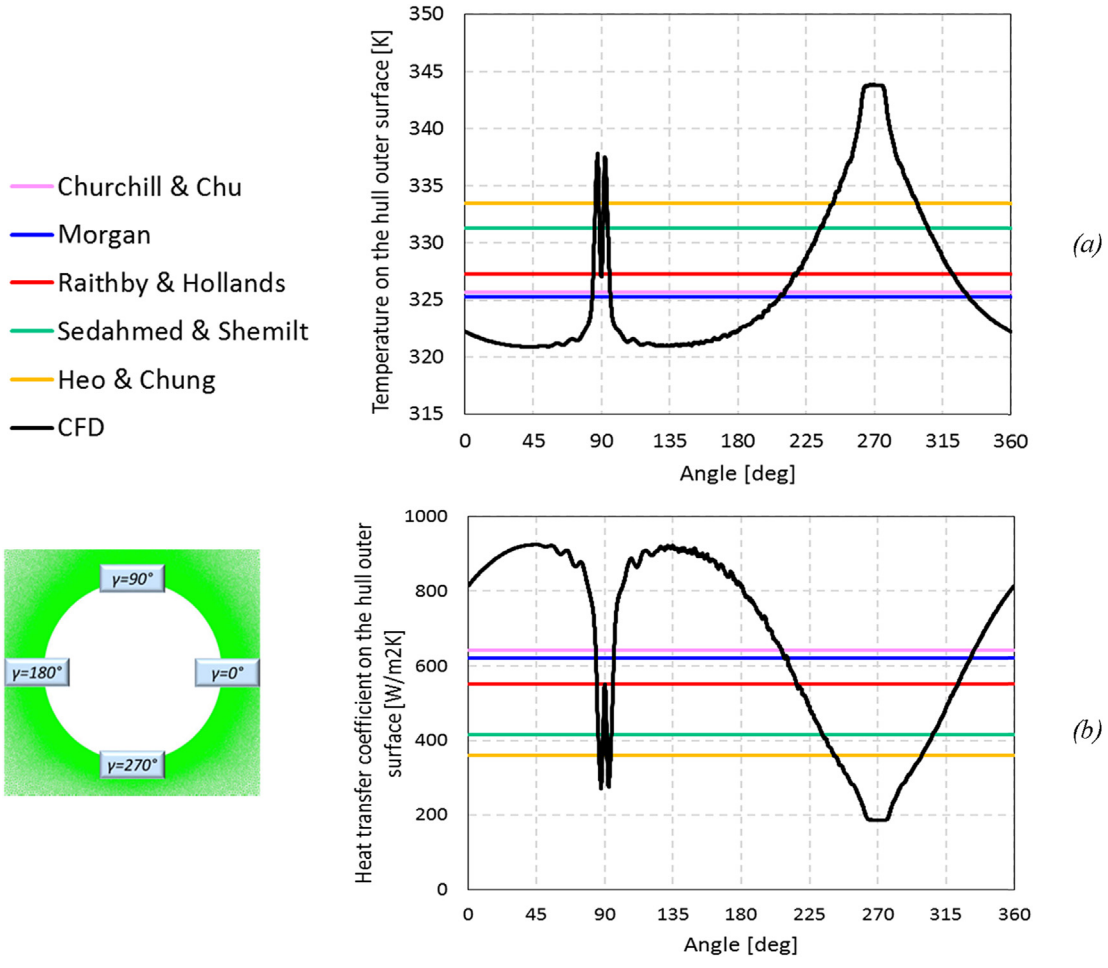

Fig. 9. Hull superficial temperature (a) and heat transfer coefficient (b) profiles on the hull outer surface.

3.4.1. Sensitivity to the mesh and discretization schemes

Sensitivity to the mesh was performed considering the number of cells, especially refining the laminar boundary layer region, and the structure of the grid. Four grids with square, triangular or hybrid structure, amount of cells ranging from 150 000 to 750 000 and y^+ of the nearest wall cell decreasing from 142 to 1.45 were tested.

Results show that, once the grid is provided with a sufficiently fine boundary layer (at least one node in the viscous sub-layer, i.e. $y^+<5$), results are not anymore sensible to the spatial discretization. In this case, very small discrepancies among the results are obtained: 0.25% for hull outer temperature, 1.7% for heat flux across the hull, 7.9% for heat transfer coefficient. However, even if the boundary layer is coarse and the y + value is very high, discrepancies are on the whole acceptable (maximum discrepancies: 0.5% on hull average outer temperature, 3.3% on average heat flux, 14.6% on global heat transfer coefficient).

Effects due to different time step size and numerical discretization schemes were found to be negligible.

3.4.2. Sensitivity to the turbulence model

It is important to perform a sensitivity analysis to the turbulence model, since up to date the modeling of turbulence in natural circulation is still a complex challenge for researchers in CFD. Sensitivity on the turbulence model was carried out by adopting other types of RANS models (i.e k-ε standard and k-ε realizable, both tested with standard wall function and enhanced wall treatment, k-ω standard), the only ones usable in a 2D simulation, and different wall treatments.

Among these, only the k-ε realizable model, used with the enhanced wall function and a very fine grid in the near wall zone (y^+ of the nearest wall node 1.45), provided results very similar to those of the reference case, as visible in Table 6.

Other models prominently underestimate or overestimate the heat flux and the heat transfer coefficient. These are believed to be not fully reliable for the case under investigation. Standard k-ε assumes isotropic turbulence structure and is believed to be inappropriate for this kind of problem where the flow velocity is not high and driven by a buoyancy force. Moreover, the use of k-ε model with the standard wall function is unsuitable for this type of flow. Consequently, because of predictions of excessive levels of turbulent shear stress, especially in stagnation regions, it gives rise to excessive heat transfer estimation. Without an adequate wall treatment, the resolution of the phenomena near the outer surface of the hull is distorted and the result is an overestimation of the heat transfer. Standard k-omega is usually not recommended, since

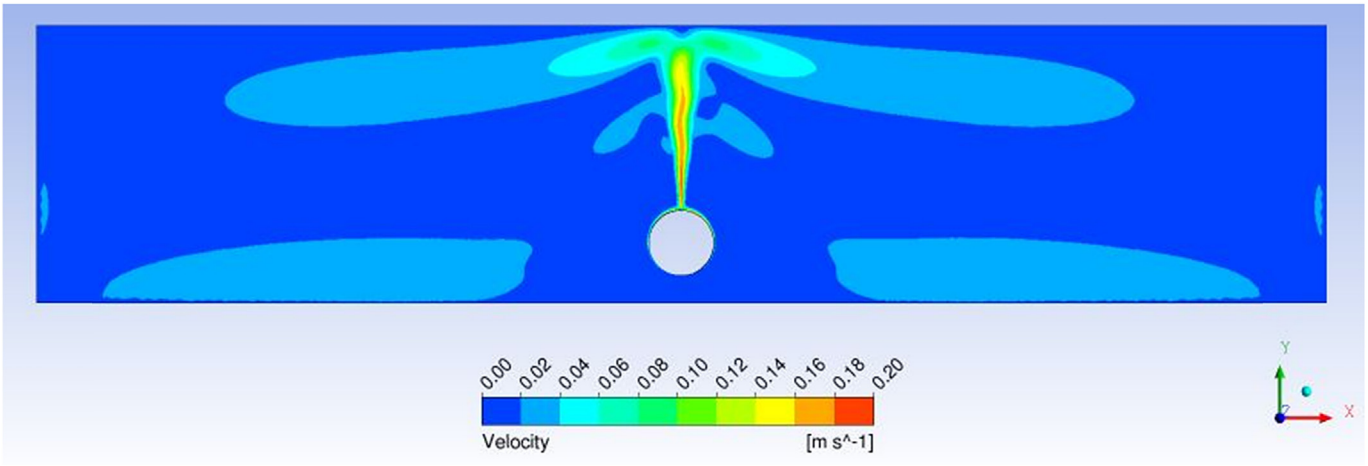

Fig. 10. Total velocity field after 8580 s.

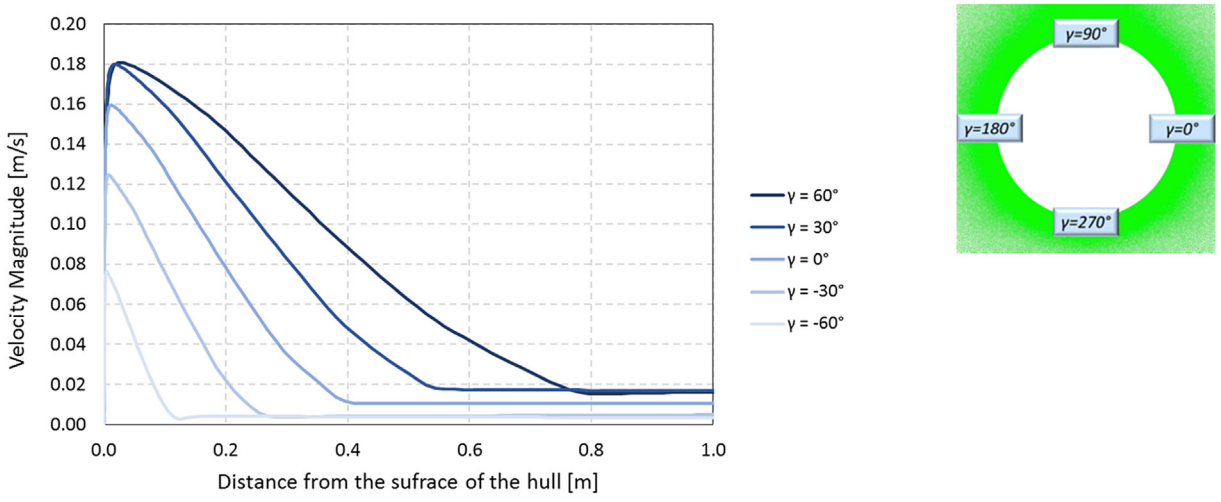

Fig. 11. Velocity boundary layer on the right side of the hull (at different angles).

the downside of the standard ω-equation is a relatively strong sensitivity of the solution depending on the freestream values of k and ω outside the shear layer.

3.5. Parametric analysis

The evaluation of the influence of several parameters on the heat transfer capacity of the hull was performed as well. CFD simulations considering different values of i) sea current, ii) immersion depth, iii) internal temperature and iv) seawater temperature were carried out. Main results are summarized in Table 7.

3.5.1. Presence of sea currents

The numerical modeling of this problem required some relevant modifications with respect to the reference case. First of all, a different grid was necessary in order to allow the visualization of the recirculation vortices behind the hull: the hull has been shifted to the left side of the region of interest, while the same approach for the boundary layer has been maintained. Then, opportune boundary conditions on the sides of the mesh have been adopted to simulate the presence of the sea current: velocity inlet condition with uniform profile on the left wall and pressure outlet condition on the right wall were assumed. In a 2D simulation only one direction of the current, i.e. horizontal crossflow, can be simulated. Finally, a time dependent boundary condition was set on the internal surface of the hull: the heating of the hull started 600 s after the beginning of the simulation, in order to allow the development of the flow and simulate a plausible transient. A total transient of 3600 s has been simulated.

The impact of cross flow sea currents, ranging from 0.01 m/s to 2 m/s, was significant, leading to a considerable enhancement of the heat transfer capabilities of the hull with respect to the reference case (stagnant water); heat transfer coefficient linearly increases up to ten times, global heat flux can be up to 33% higher. This situation is shown in Fig. 13 and results are reported in Table 8. Fig. 14 shows temperature and velocity fields of the case with sea

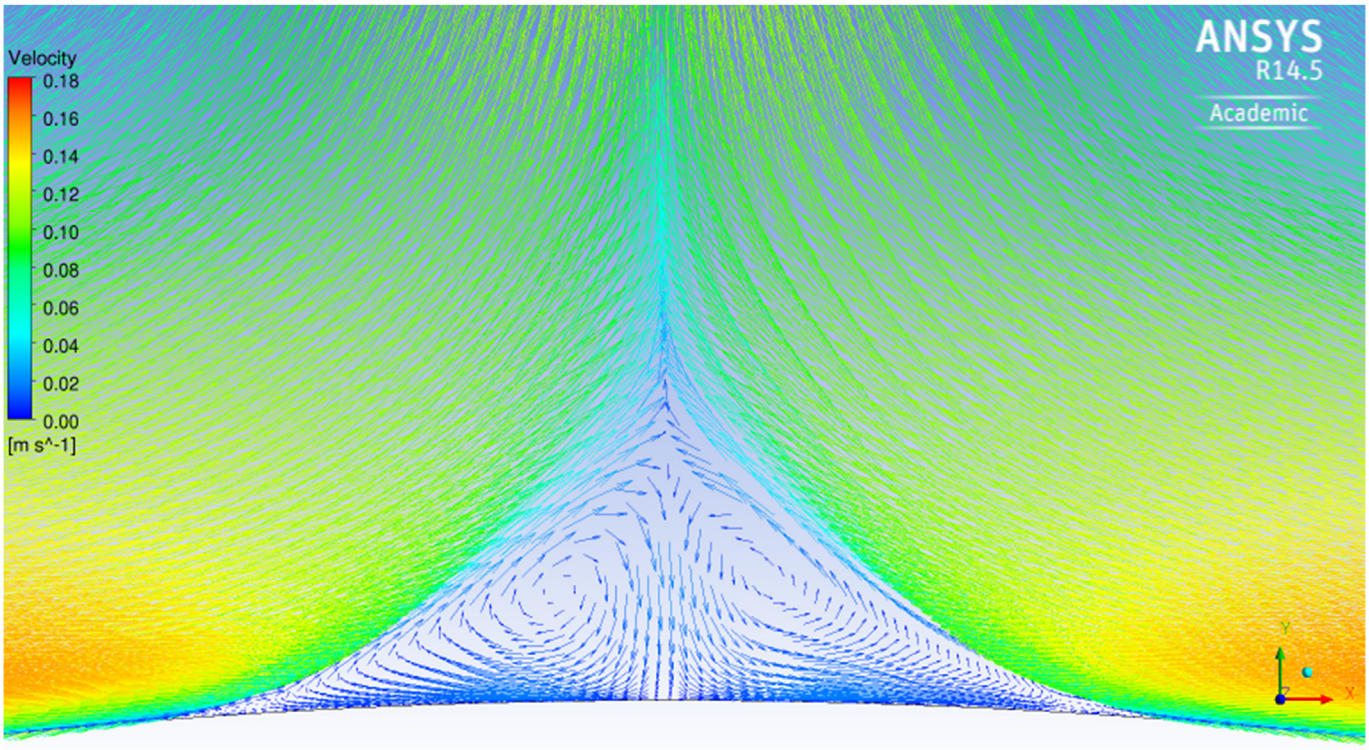

Fig. 12. Velocity vectorial plot of the region near the summit of the hull.

Table 6
Results of the sensitivity analysis – Turbulence model k-ε realizable.

Turbulence model	Hull outer surface average temperature [K]	Average heat flux [W/m^2]	Average heat transfer coefficient [W/m^{2}K]
k-ε realizable with enhanced wall treatment and nearest wall cell $y^+ = 1.45$	327.0	10 514	630.1
SST k-ω with nearest wall cell $y^+ = 4.92$ (Reference Case)	326.2	10 686	670.7

Table 7
Summary of the parametric analysis (in brackets: discrepancy with respect to the reference case in Table 5).

Parameter	Reference value	Parametric analysis	Global heat flux [W/m^2]	Global heat transfer coefficient [W/m^{2}K]
Sea current velocity	0 m/s	0.01 m/s – 2 m/s	11 004–14 237 (+3%, +33%)	700.6–8438.9 (+4.5%, +1159%)
Immersion depth	60 m	100 m	10 679 (no discrepancy)	677.7 (no discrepancy)
Hull internal temperature	100 °C	180 °C	24 091 (+140%)	914.7 (+36%)
Seawater temperature	35 °C	10 °C	13 569 (+27%)	497.3 (−25%)

current velocity equal to 0.2 m/s.

3.5.2. Hull internal temperature

The temperature on the internal hull surface is for sure one of the most critical boundary condition of the reference model. The reference case considers uniform temperature of 100 °C on the hull internal surface, corresponding to saturation pressure of one bar inside the containment. It is very likely that, during an accident scenario, internal pressure, and consequently internal temperature, would reach greater values, leading to a sensible enhancement of heat transfer with respect to the reference case.

The parametric analysis revealed that, if internal temperature is equal to 180 °C (i.e. 10 bars of internal saturation pressure), the global heat flux is more than two times higher and the heat transfer coefficient is nearly 35% greater. Results are reported in Table 9. The total decay power that can be rejected by the hull under these conditions is therefore much greater.

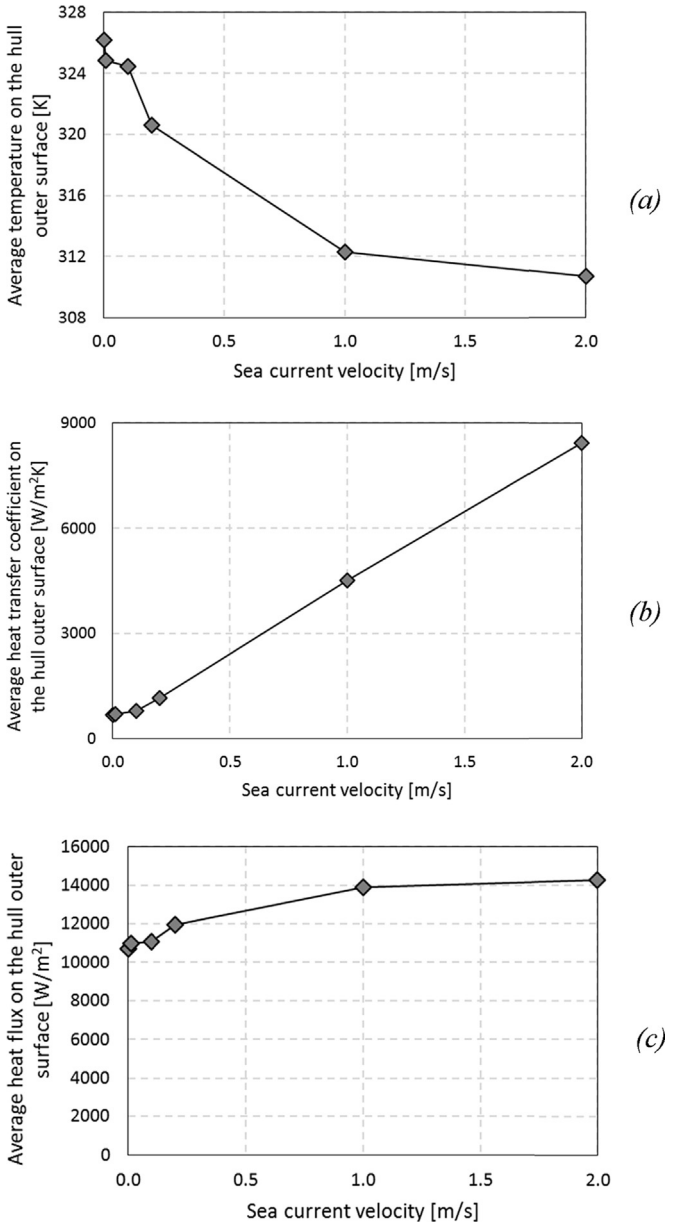

Fig. 13. Average hull superficial temperature (a), global heat transfer coefficient (b) and global heat flux (c) as a function of the sea current velocity.

3.5.3. Seawater temperature

If seawater temperature is lower than that of the reference case, one can think that in principle heat transfer improves, since the temperature difference between the hull outer surface and the undisturbed seawater increases. Nevertheless, thermo-physical properties of seawater are dependent on temperature and their variation can significantly affect the heat transfer process. In particular, the effect of viscosity is the most relevant, since it can be doubled by a reduction of 25 °C in temperature.

In the parametric analysis, a CFD simulation considering seawater temperature equal to 10 °C has been performed. Results show that colder seawater reduces the hull outer surface temperature and increases heat flux. However, the higher viscosity of colder water reduces the global heat transfer coefficient, which is considerably lower with respect to the reference case. Numerical values are reported in Table 10.

3.6. Application of the results to the Flexblue® geometry

In the Flexblue® reference design, the drywell is 25 m long with a 14 m diameter. That means that the Flexblue® drywell hull area in contact with seawater is about 1100 m^2. In the reference case of this study, considering the very simplified hypothesis of a uniform temperature of 100 °C along the internal side of the drywell (e.g. consequently to a large break loss of coolant accident), the global heat flux rejected to seawater will be 11.75 MW. This value corresponds to the residual decay heat of Flexblue® core 20 min after the shutdown. This study is not sufficient to obtain an ultimate result about the heat transfer capacities of the hull, because more investigations are needed (especially a study of the internal heat transfer and an experimental validation of the numerical results), but it shows the great potential of the Flexblue® design to remove residual power to the heat sink.

4. Conclusions

The study on the Flexblue® hull external fluid dynamics in natural circulation conditions revealed that available heat transfer correlations lead to scattered results, when the hull heat rejection capabilities are evaluated. The main reason is that Flexblue® hull uncommon dimensions correspond to Rayleigh numbers falling outside the range of validity of those empirical correlations for

Table 8
Results of the parametric analysis – presence of sea currents.

Sea current velocity [m/s]	Hull outer surface average temperature [K]	Average heat flux [W/m^2]	Average heat transfer coefficient [W/m^2K]
0.01	324.8	11 004	700.6
0.1	324.5	11 091	806.1
0.2	320.6	11 972	1159.3
1.0	312.3	13 871	4512.5
2.0	310.7	14 237	8438.9
0.0 (Reference Case)	326.2	10 686	670.7

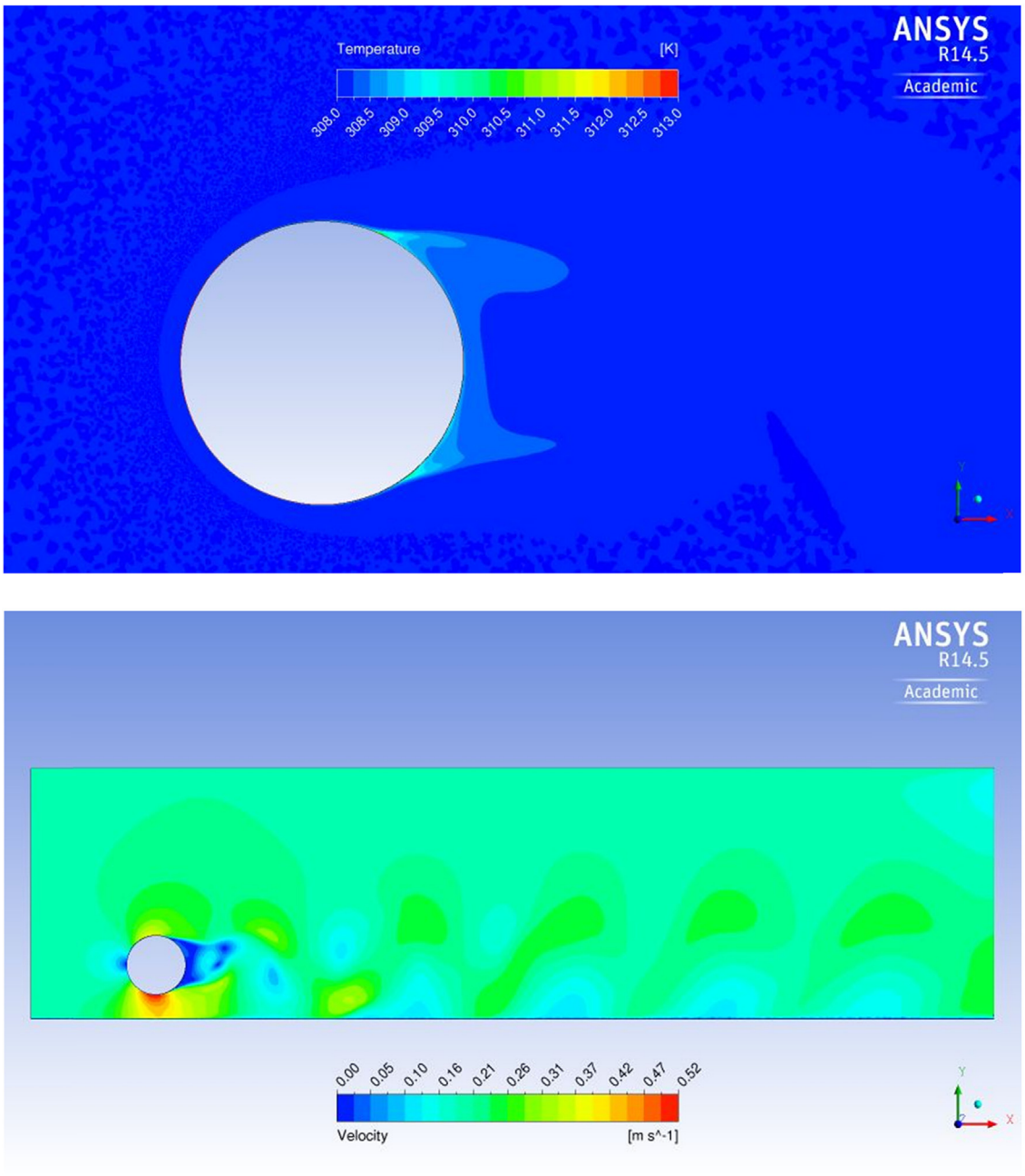

Fig. 14. Temperature (a) and velocity (b) fields of the case with sea current velocity equal to 0.2 m/s (time 3600 s).

Table 9
Results of the parametric analysis – Internal temperature.

Internal temperature [K]	Hull outer surface average temperature [K]	Average heat flux [W/m^2]	Average heat transfer coefficient [W/m^{2}K]
453	340.5	25 697	914.6
373 (Reference Case)	326.2	10 686	670.7

Table 10
Results of the parametric analysis – Seawater temperature.

Seawater temperature [K]	Hull outer surface average temperature [K]	Average heat flux [W/m^2]	Average heat transfer coefficient [W/m^{2}K]
283	313.6	13 569	497.3
308 (Reference Case)	326.2	10 686	670.7

cylindrical geometry, usually based on experimental data referred to tubes or piping of limited diameters. Meanwhile, an approximated approach based on planar surfaces necessarily requires very strong and nearly unphysical assumptions. Hence, approaches based on existing empirical correlations are not suitable for the current problem. The 2-D CFD preliminary analysis carried out to better investigate the phenomenon led to heat transfer coefficient values larger than the largest obtained through the correlations, thus confirming that their adoption to estimate the decay heat removal capability would not be reliable. An internal hull temperature of 100 °C in a stagnant seawater environment at 35 °C yields an average heat flux of 10.7 MW/m^2, which corresponds to the decay heat of Flexblue 20 min after shutdown. The presence of a weak sea current as well as a colder seawater temperature significantly improves heat transfer, which highlights the conservatism of the assumptions.

A 3-D CFD analysis will be performed as a further step in the investigation. Moreover, a large scale experimental study is mandatory to support the heat transfer correlations and to validate the CFD approach.

Aknowledgments

The authors would like to express their gratitude to prof. Fabio Inzoli and Dr. Riccardo Mereu of CFDLab@Energy – Department of Energy of Politecnico di Milano, who provided very precious suggestions and technical support.

Nomenclature

Latin letters

c_p	specific heat
D	diameter
g	gravity constant
G	generation term
h	heat transfer coefficient
K	thermal conductivity
k	turbulent kinetic energy
Nu	Nusselt number $Nu = \frac{hD}{k}$
q”	heat flux
p	pressure
Pr	Prandtl number $Pr = \frac{\mu c_p}{k}$
Ra	Rayleigh number $Ra = \frac{g\beta\rho^2 c_p (T_w - T_\infty) D^3}{\mu K}$
T	temperature
t	time
u	horizontal component of fluid velocity
v	vertical component of fluid velocity
x	horizontal coordinate
y	vertical coordinate
Y	dissipation term

Greek letters

β	thermal expansion coefficient
μ	dynamic viscosity
ρ	density
σ	turbulent Prandtl number
φ	plate inclination
ω	turbulent dissipation rate

Subscripts

bio	biofouling layer
ext	external
L	local
l	laminar
p	paint layer
sea	seawater
steel	steel layer
t	turbulent
w	wall

APPENDIX A

Heat transfer correlations adopted in the analysis.

Authors	Correlations
Morgan (Morgan, 1975)	$\overline{Nu_D} = CRa_D^n$

Ra_D	C	n
10^{-10} - 10^{-2}	0.675	0.058
10^{-2} - 10^{2}	1.02	0.148
10^{2}–10^{4}	0.850	0.188
10^{4}–10^{7}	0.480	0.250
10^{7}–10^{12}	0.125	0.333

Churchill and Chu (Churchill and Chu, 1975a)	$\overline{Nu_D} = \left\{ 0.60 + \frac{0.387 Ra_D^{1/6}}{\left[1+\left(\frac{0.559}{Pr}\right)^{9/16}\right]^{8/27}} \right\}^2$ for $Ra_D \le 10^{12}$
Sedahmed and Shemilt (Sedahmed and Shemilt, 1982)	$\overline{Nu_L} = 0.498(Ra_L \cos\varphi)^{0.28}$
Heo and Chung (Heo and Chung, 2012)	*Laminar flow:* $\overline{Nu_D} = 0.3 Ra_D^{0.25}(1 + 0.7\cos\varphi)$ *Turbulent flow:* $\overline{Nu_D} = 0.13 Ra_D^{0.3}(1 + 0.6\cos\varphi)$
Raithby and Hollands (Raithby and Hollands, 1998)	$\overline{Nu}^T = 0.772\overline{C}_l Ra_D^{0.25}\overline{Nu}_l = \frac{2f}{\ln\left(1+\frac{2f}{\overline{Nu}^T}\right)}$; $\overline{Nu_t} = \overline{C}_t Ra_D^{1/3}\overline{Nu_D} = [(\overline{Nu_l})^m + (\overline{Nu_t})^m]^{1/m}$ with $m \approx 10$

Constant	Pr = 0.7	Pr = 6	Pr = 100	Pr = 2000
C_l	0.515	0.608	0.656	0.668
C_t	0.103	0.109	0.097	0.088

References

Awad, M.M., 2011. In: Belmiloudi, Aziz (Ed.), Heat Transfer - Theoretical Analysis, Experimental Investigations and Industrial Systems Surfaces. InTech.

Boarin, S., et al., 2012. Financial case studies on small and medium-size modular reactors. Nucl. Technol. 178 (2), 218.

Braga Vieira, C., Alves Romero, G., Su, J., 2010. Computational simulation of natural convection of a molten core in lower head of a PWR pressure vessel. Uberlândia, MG, Brazil, Proc. 13th Braz. Congr. Therm. Sci. Eng. 1–8. http://www.iaea.org/inis/collection/NCLCollectionStore/_Public/42/056/42056470.pdf.

Buongiorno, J., Jurewicz, J., Golay, M., Todreas, N., 2016. The offshore floating nuclear plant (OFNP) concept. Nucl. Technol. 194, 1–14.

Churchill, S.W., Chu, H.H.S., 1975a. Correlating equations for laminar and turbulent free convection from a horizontal cylinder. Int. J. Heat Mass Transf. 18 (9).

Churchill, S.W., Chu, H.H.S., 1975b. Correlating equations for laminar and turbulent free convection from a vertical plate. Int. J. Heat Mass Transf. 18 (11).

Clausing, A.M., Berton, J.J., 1989. An experimental investigation of natural convection from an isothermal horizontal plate. ASME J. Heat Transf. 904–908.

Fujii, T., Imura, H., 1972. Natural-convection heat transfer from a plate with arbitrary inclination. Int. J. Heat Mass Transf. 15 (4).

Ganguli, A.A., Sathe, M.J., Pandit, A.B., Joshi, J.B., Vijayan, P.K., 2010. Hydrodynamics and heat transfer characteristics of passive decay heat removal systems: CFD simulations and experimental measurements. Chem. Eng. Sci. 65, 3457–3473.

General Dynamics Electric Boat Division, 1971. Potential Environmental Effects of an Offshore Submerged Nuclear Power Station. Program 16130 GFI report for the Water Quality Research Office of the Environmental Protection Agency.

Haratyk, G., Lecomte, C., Briffod, F.-X., 2014. Flexblue®: a Subsea and Transportable Small Modular Power Plant. Proc. of ICAPP 2014, Charlotte, USA.

Heo, J.H., Chung, B.J., 2012. Natural convection heat transfer on the outer surface of inclined cylinders. Chem. Eng. Sci. 73.

ANSYS FLUENT Theory Guide, ANSYS Inc. Release 14.0, (2011).

Herring, J.S., 1993. Submerged passively-safe power plant. U. S. Pat. 5 (247), 553.

Jeong, H.M., Lee, Y.H., Ji, M.K., Bae, K.Y., Chung, H.S., 2009. Natural convection heat transfer estimation from a longitudinally finned vertical pipe using CFD. J. Mech. Sci. Technol. 23, 1517–1527.

Kader, B., 1981. Temperature and concentration profiles in fully turbulent boundary layers. Intternational J. Heat Mass Transf. 24 (9), 1541–1544.

Kessides, I.N., 2012. The future of the nuclear industry reconsidered: risks, uncertainties, and continued promise. Energy Policy 48, 185.

Kitamura, K., Kimura, F., 1995. Heat transfer and fluid flow of natural convection adjacent to upward-facing horizontal plates. Int. J. Heat Mass Transf. 38.

Kozanoglu, B., Lopez, J., 2007. Thermal boundary layer and the characteristic length on natural convection over a horizontal plate. Heat Mass Transf. 43.

Krepper, E., Koncar, B., Egorov, Y., 2007. CFD modelling of subcooled boiling: concept, validation and application to fuel assembly design. Nucl. Eng. Des. 237, 716–731.

Kuznetsov, V., 2012. Marine Derivative Light Water Reactor Concepts: Barge-mounted and Seabed-based Plants. Proc. of the F. Joliot and O. Hahn Summer School (FJOH 2012). CEA-KIT, Aix-en- Provence, France.

Lokhov, A., et al., 2011. OECD/NEA study on the economics and market of small reactors. Nucl. Eng. Technol. 45 (6), 701.

McAdams, W.H., 1954. Heat Transmission. Chemical engineering series. McGraw-Hill.

Menter, F.R., 1994. Two-equation eddy-viscosity turbulence models for engineering applications. Am. Inst. Aeronautics Astronautics J. 32, 8.

Morgan, V.T., 1975. The Overall Convective Heat Transfer from Smooth Circular Cylinders. Advances in Heat Transfer 11. Academic press, New York.

Pugh, S., Hewitty, G.F., Muller-Steinhagenz, H., 2003. Fouling during the Use of Seawater as Coolant - the Development of a User Guide. ECI Digital Archives.

Raithby, G.D., Hollands, K.G.T., 1998. Handbook of Heat Transfer Fundamental (Chapter 4). McGraw-Hill Book Company, New York.

Ramana, M.V., et al., 2013. Licensing small modular reactors. Energy 61, 555.

Rosner, R., Goldberg, S., 2011. Small Modular Reactors – Key to Future Nuclear Power in the U.S.. DOE technical paper, (chapter 4) University of Chicago Energy Policy Institute, Illinois.

Sedahmed, G.H., Shemilt, L.W., 1982. Natural convection mass transfer at cylinders in different positions. Chem. Eng. Sci. 37 (2).

Thomas, S., 2012. What will the Fukushima disaster change? Energy Policy 45, 12.

Vujic, J., et al., 2012. Small modular reactors: simpler, safer, cheaper. Energy 45, 288.

Xie, Y., 2012. TVA's small reactor project faces delay. Nucleon. Week 53 (12), 1.